AJNR

Progressive Changes in Cerebral Apparent Diffusion Values in Fabry Disease: A 5-Year Follow-up MRI Study

Koen P.A. Baas, Albert J. Everard, Simon Körver, Laura van Dussen, Bram F. Coolen, Gustav J. Strijkers, Carla E.M. Hollak and Aart J. Nederveen

AJNR Am J Neuroradiol published online 28 September 2023
http://www.ajnr.org/content/early/2023/09/28/ajnr.A8001

Published September 28, 2023 as 10.3174/ajnr.A8001

Progressive Changes in Cerebral Apparent Diffusion Values in Fabry Disease: A 5-Year Follow-up MRI Study

Koen P.A. Baas, Albert J. Everard, Simon Körver, Laura van Dussen, Bram F. Coolen, Gustav J. Strijkers, Carla E.M. Hollak, and Aart J. Nederveen

ABSTRACT

BACKGROUND AND PURPOSE: White matter lesions are commonly found in patients with Fabry disease. Existing studies have shown elevated diffusivity in healthy-appearing brain regions that are commonly associated with white matter lesions, suggesting that DWI could help detect white matter lesions at an earlier stage This study explores whether diffusivity changes precede white matter lesion formation in a cohort of patients with Fabry disease undergoing yearly MR imaging examinations during a 5-year period.

MATERIALS AND METHODS: T1-weighted anatomic, FLAIR, and DWI scans of 48 patients with Fabry disease (23 women; median age, 44 years; range, 15–69 years) were retrospectively included. White matter lesions and tissue probability maps were segmented and, together with ADC maps, were transformed into standard space. ADC values were determined within lesions before and after detection on FLAIR images and compared with normal-appearing white matter ADC. By means of linear mixed-effects modeling, changes in ADC and ΔADC (relative to normal-appearing white matter) across time were investigated.

RESULTS: ADC was significantly higher within white matter lesions compared with normal-appearing white matter ($P < .01$), even before detection on FLAIR images. ADC and ΔADC were significantly affected by sex, showing higher values in men (60.1 [95% CI, 23.8–96.3] $\times 10^{-6}$mm^2/s and 35.1 [95% CI, 6.0–64.2] $\times 10^{-6}$mm^2/s), respectively. ΔADC increased faster in men compared with women (0.99 [95% CI, 0.27–1.71] $\times 10^{-6}$mm^2/s/month). ΔADC increased with time even when only considering data from before detection (0.57 [95% CI, 0.01–1.14] $\times 10^{-6}$mm^2/s/month).

CONCLUSIONS: Our results indicate that in Fabry disease, changes in diffusion precede the formation of white matter lesions and that microstructural changes progress faster in men compared with women. These findings suggest that DWI may be of predictive value for white matter lesion formation in Fabry disease.

ABBREVIATIONS: ERT = enzyme replacement therapy; IQR = interquartile range; LME = linear mixed effect; MNI = Montreal Neurological Institute; NAWM = normal-appearing white matter; TP = time point; WML = white matter lesion

Fabry disease is a rare, X-linked lysosomal storage disorder caused by a mutation in the galactosidase alpha (*GLA*) gene.[1] This mutation causes a deficiency of α-galactosidase A activity, resulting in the accumulation of glycosphingolipids, mainly globotriaosylceramide, primarily in the cardiovascular system, brain, and kidneys.[2] Accumulation in the arterial walls is believed to contribute to cerebrovascular and cardiac diseases, which are among the leading causes of death in patients with Fabry disease. Among other neurologic findings, white matter lesions (WMLs) are found in nearly one-half of all patients.[3-5] WML burden increases with age and is associated with cognitive decline.[5,6] Although the prevalence, severity, and progression of WMLs are comparable in men and women, men develop WMLs at a younger age.[4,7] Moreover, a higher prevalence of WMLs in men with classic compared with nonclassic Fabry disease has been reported.[8]

The pathophysiology of WMLs in Fabry disease is complex and incompletely understood. Cell damage in the cerebrovascular system may impair the autoregulation of cerebral perfusion, resulting in a hyperdynamic circulation and endothelial dysfunction caused by shear stress and incompliant vessel walls.[4,9,10] Combined with glycosphingolipid storage in endothelial cells, these effects might cause the release of reactive oxygen species, further compromising

Received May 3, 2023; accepted after revision August 16.

From the Departments of Radiology and Nuclear Medicine (K.P.A.B., A.J.N.), Endocrinology and Metabolism (S.K., L.v.D., C.E.M.H.), and Biomedical Engineering and Physics (B.F.C., G.J.S.), Amsterdam University Medical Centers, University of Amsterdam, Amsterdam, the Netherlands; Faculty of Science (A.J.E.), Vrije Universiteit Amsterdam, Amsterdam, the Netherlands; and Amsterdam Cardiovascular Sciences (B.F.C., G.J.S.), University of Amsterdam, Amsterdam, the Netherlands.

Please address correspondence to Aart J. Nederveen, PhD, Department of Radiology and Nuclear Medicine, Amsterdam University Medical Centers, University of Amsterdam, Meibergdreef 9, 1105 AZ, Amsterdam, the Netherlands; e-mail: a.j.nederveen@amsterdamumc.nl

Indicates article with online supplemental data.

http://dx.doi.org/10.3174/ajnr.A8001

endothelial cells and accelerating vascular dysfunction.[11,12] Patients with Fabry disease with and without WMLs have shown increased CBF but decreased glucose metabolism in the WM, indicating microangiopathy.[13] Last, increased CSF protein levels have been reported, indicating blood-brain barrier dysfunction.[14]

MR imaging is the criterion standard imaging technique to detect brain alterations in Fabry disease, including WMLs. DWI can accurately quantify microstructural WM changes and has been used in patients with Fabry disease.[5,15,16] These studies showed elevated mean diffusivity in healthy-appearing brain regions that are commonly associated with WMLs.[5,15,16] Moreover, WM mean diffusivity was found to be correlated with plasma globotriaosylceramide levels.[5] These findings suggest that DWI could help to detect WML formation at an earlier stage and potentially provide a tool to evaluate treatment options like enzyme replacement therapy (ERT). However, these studies were of a cross-sectional design, prohibiting the assessment of longitudinal changes required to investigate whether changes in diffusion precede WML formation. Therefore, this study aimed to explore whether DWI can detect microstructural changes before WMLs appear on FLAIR-weighted images in a cohort of patients with Fabry disease undergoing yearly MR imaging examinations during a 5-year period.

MATERIALS AND METHODS

For this retrospective, observational study, we adhered to the guidelines of the STrengthening the Reporting of OBservational studies in Epidemiology (STROBE) statement. Data collection has been described before.[17] The Amsterdam University Medical Centers (location in the Academic Medical Center) are the national referral center for patients with Fabry disease in the Netherlands. Follow-up at the outpatient clinic ranged from 6 months to once every 2 years and included brain MR imaging scans. Follow-up data from patients with a confirmed Fabry disease diagnosis were collected in a local database after patients provided written informed consent. From this database, follow-up data collected between 2013 and 2019 were extracted. All patients were classified as having the classic or nonclassic phenotype using predefined criteria.[8,18,19] Patients were included if good-quality FLAIR-weighted, T1-weighted, and DWI scans from at least 3 visits were available. According to Dutch law, no approval of the study protocol was needed because this was a retrospective study and patients were not subjected to procedures or rules of behavior in addition to regular clinical follow-up.

Image Acquisition

MR imaging scans were acquired on 3T scanners (Ingenia; Philips Healthcare). T1-weighted anatomic scans were acquired with the following parameters: TR/TE: 9/4.1 ms, flip angle: 8°, resolution: 0.5 × 0.5 × 0.9 mm^3, FOV: 256 × 256 × 170 mm^3, and number of averages: 1. DWI scans were acquired with 2 b-values, 0 and 1000 s/mm^2. Other acquisition parameters were the following: TR/TE: 6340/83 ms, flip angle: 90°, resolution: 0.9 × 0.9 × 3.0 mm^3, FOV: 229 × 229 ×147 mm^3, and number of averages: 2. FLAIR acquisition parameters were as follows: TR/TE: 4800/356 ms, flip angle: 90°, resolution: 1.04 × 1.04 × 1.12 mm^3, FOV: 250 × 250 × 360 mm^3, and number of averages: 2. MR imaging software upgrades introduced some variation in acquisition parameters of the DWI scan (Online Supplemental Data). Periodic image-quality tests using a vendor-provided phantom were performed during the course of the study, including before and after software upgrades. Any observed abnormalities were addressed by the vendor before continuation. Patient positioning and planning of the scans were performed according to standard clinical procedures. FLAIR scans were assessed by a neuroradiologist for WMLs according to the Fazekas scale. The Fazekas scale rates WMLs in the periventricular and deep brain separately from zero (no WMLs) to 3 (severe confluent WMLs) and adds both scores, resulting in a total score that can range from zero to 6.

Postprocessing

Postprocessing was performed in Matlab (Version 2019b; MathWorks). An overview of the processing steps is schematically shown in Fig 1.

T1-weighted scans were segmented into GM, WM, and CSF probability maps using CAT12 (https://neuro-jena.github.io/cat12-help/) and nonlinearly registered to standard Montreal Neurological Institute (MNI) space using SPM12 (http://www.fil.ion.ucl.ac.uk/spm/software/spm12) (Fig 1*A*). After registration to MNI space, tissue probability maps were thresholded at 0.8.

WMLs were automatically segmented on the FLAIR images using the lesion segmentation toolbox (https://www.applied-statistics.de/lst.html) lesion-prediction algorithm[20] and manually corrected (Fig 1*B*). This segmentation was performed only on FLAIR images that were scored >0 on the Fazekas score to avoid false-positive detections. WML probability maps were thresholded at 0.2, which was deemed appropriate on the basis of visual inspection (Online Supplemental Data). Corrected WML maps were registered to MNI space.

ADC maps were fitted from the DWI data using the FMRIB Software Library (https://fsl.fmrib.ox.ac.uk/fsl/fslwiki/) (Fig 1*C*) and registered to MNI space using the previously obtained transformation matrix.

After transformation to MNI space, normal-appearing white matter (NAWM) was defined by subtracting the WML masks of every available time point (TP) from the WM masks (Fig 1*D*). WML and NAWM masks were eroded by 1 voxel, and 3-voxel dilated GM and CSF masks were subtracted from the resulting masks to prevent partial volume effects. Unconnected lesions of <5 voxels were excluded (not shown). The resulting lesion masks were termed "full lesion." Additionally, masks were created that included only WMLs that developed between 2 study visits, denoted as "new lesion." New lesion masks were created by subtracting the single-voxel dilated full lesion masks from all previous TPs from the current full lesion mask. Again, lesions of <5 voxels were excluded.

The median ADC within the created masks was calculated at each TP (before and after the first appearance on FLAIR-weighted images; Online Supplemental Data). Naming conventions as in the Online Supplemental Data will be used. The TP of first detection on a FLAIR-weighted image was defined the reference TP (time = 0) for that ROI, to which all ADC values were temporally shifted. The difference between ADC within WMLs and NAWM (ΔADC) was calculated by subtracting the median ADC within the NAWM from the lesion ADC.

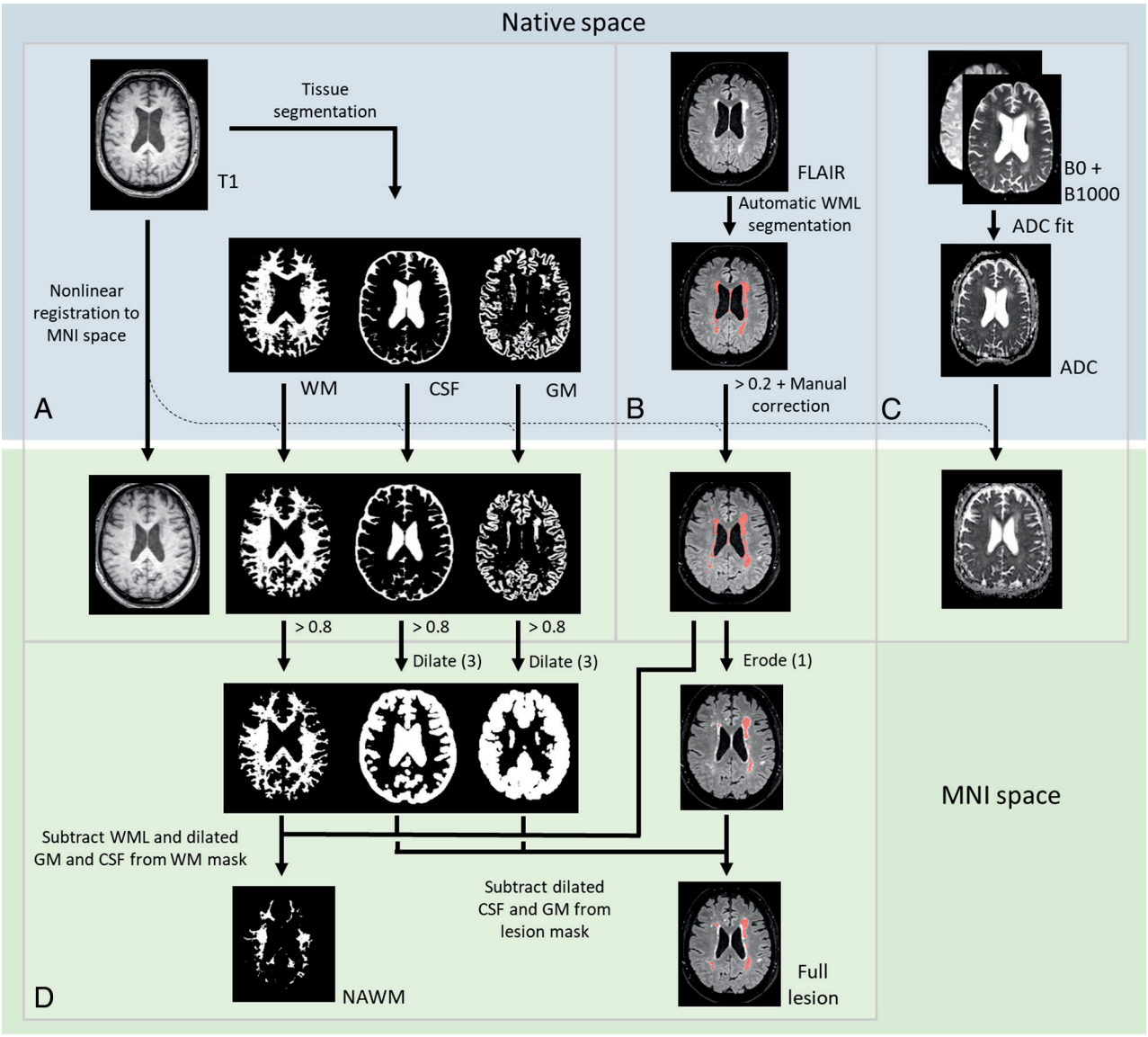

FIG 1. Overview of postprocessing steps. T1-weighted scans were segmented in native space and registered to MNI space (*A*). WMLs were automatically segmented on FLAIR images, thresholded, and manually corrected (*B*). ADC maps were fitted from DWIs with b-value = 0 and 1000 s/mm^2 (*C*). WML masks and ADC maps were registered to MNI space using the transformation matrix from the T1 registration. NAWM masks were created by subtracting the WML masks from the WM segmentation (*D*). WML masks were eroded with 2 voxels. Last, GM and CSF masks were dilated with 3 voxels and subtracted from the resulting WML mask and NAWM mask.

Statistical Analysis

Statistical analyses were performed in R Studio (Version 2022.2.3.492; http://rstudio.org/download/desktop). Descriptive statistics are reported as mean (SD) or median and interquartile range (IQR) if not normally distributed. ADC values within full and new lesions were compared with corresponding NAWM ADC values using 2-tailed paired *t* tests with a Bonferroni multiple comparison correction.

Linear mixed effect (LME) modeling was used to investigate changes in ADC and ΔADC with time.[21] This investigation was only for new lesions because the age of lesions originating from before the first MR imaging scan was unknown. Subjects were assigned as the random effect and TP of lesion segmentation as a crossed random effect to account for multiple TPs per patient and multiple lesion segmentations per patient, respectively.[22] The random effects structure was determined for each model separately as described in the Online Supplemental Data. Next, a priori–determined fixed and interaction effects were added. Fixed effects included time (in months, respectively, to the reference point), sex, and age. Age at baseline was used and centered around the mean. Finally, interaction effects between time and sex and between time and age were included.

$$ADC \sim Time + Sex + Age_{baseline} + (Time|Subject)$$
$$+(1|TP_{seg}) + Time : Sex + Time : Age_{baseline}.$$

If the model could not converge, the structure was simplified as described in the Online Supplemental Data. Model assumptions

Table 1: Patient characteristics and WML scores

	All	Men	Women
Patient characteristics			
No. of patients (%)	48	25 (52%)	23 (48%)
Classic phenotype (No.) (%)	48 (100%)	25 (100%)	23 (100%)
No. of scan data sets (No.)	229	117	112
Age at first MR imaging (median) (range) (yr)	44 (15–69)	31 (15–55)	46 (22–69)
Patients <18 yr (No.) (%)	2 (4.2%)	2 (8.0%)	0 (0.0%)
Ever ERT (No.) (%)	48 (100%)	25 (100%)	23 (100%)
Months treated (mean)	89 (SD, 34)	92 (SD, 39)	86 (SD, 30)
Events before first MR imaging			
Cerebrovascular event (No.) (%)	2 (4.2%)	1 (4.0%)	1 (4.3%)
TIA (No.) (%)	1 (2.1%)	1 (4.0%)	0 (0.0%)
Kidney function at first MR imaging			
eGFR in mL/min/1.73 m^2 (median) (range)	101 (40–154)	105 (49–154)	100 (40–127)
eGFR <60 mL/min/1.73 m^2 (No.) (%)	5 (10.4%)	3 (12%)	2 (8.7%)
WML scores			
Fazekas first MR imaging (median) (range)	1 (0–6)	0 (0–6)	1 (0–6)
Fazekas first MR imaging (mean)	1.5 (SD, 1.7)	1.4 (SD, 2.0)	1.5 (SD, 1.3)
Fazekas > 0 first MR imaging (No.) (%)	29 (60%)	11 (44%)	18 (78%)
Fazekas last MR imaging (median) (range)[a]	1 (0–6)	1 (0–6)	1 (0–6)
Fazekas last MR imaging (mean)	1.5 (SD, 1.6)	1.6 (SD, 1.9)	1.4 (SD, 1.3)
Fazekas > 0 last MR imaging (No.) (%)	33 (69%)	15 (60%)	18 (78%)

Note:—eGFR indicates estimated glomerular filtration rate.
[a] For 32 patients, additional MR imaging after Fazekas scoring was performed. For these patients, the last known Fazekas score was used.

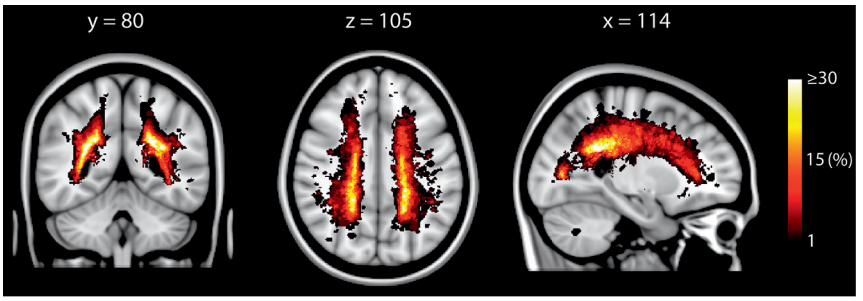

FIG 2. Lesion prevalence in patients with Fabry disease. Y, Z, and X coordinates refer to standard MNI space.

were tested by fitting of the residuals against the observed data and inspecting their normality. Estimated effects and their 95% CIs are reported.

Models were also evaluated using only the ADC values before detection on FLAIR-weighted images (time < 0). To investigate NAWM ADC in patients with and without lesions, we included a grouping variable "presence of lesions" as a fixed effect, indicating whether WMLs, at any TP, had been found in a patient.

Data Availability

Data are available on reasonable request but not publicly available. Because of the rarity of the disease, even anonymized data can be linked to a specific individual.

RESULTS

Data from 49 patients with Fabry disease initially fulfilled the inclusion criteria. Five FLAIR scans and three T1 scans were excluded because of artifacts detected during image analysis, leading to the exclusion of 1 patient because <3 complete TPs were available. After exclusion, 48 patients with Fabry disease (23 women, all classic phenotypes, all on ERT) with a median of 5 TPs (range, 3–6 TPs) were left, totaling 229 included scan data sets (Table 1). The median interval between TPs was 364 days (range, 196–1134 days). At baseline, 29 (60%) patients had WMLs (18 women; median age, 49 years; range, 21–69 years). Four patients without WMLs at baseline developed WMLs during the study, totaling 33 (69%) patients (18 women; median age, 47 years; range, 21–69 years) who had WMLs by the end of the study. In patients who had lesions at baseline, lesion volume increased significantly during the study (median, 0.6 [IQR, 1.6] mm^3 and 1.05 [IQR, 3.1] mm^3; $Z = 15$, $P < .01$).

WMLs were predominantly found in the periventricular WM (Fig 2). At time point 1 (TP1), the mean ADC within NAWM was 765 (SD, 32) $\times 10^{-6}$ mm^2/s compared with 1113 (SD, 138) $\times 10^{-6}$ mm^2/s ($t[24] = -14$, $P < .01$) within the full lesion at that TP (full lesion TP1). ADC within full lesion ROIs from all TPs are shown in the Online Supplemental Data.

When we combined new lesion ADC values with the same time respective to their reference point, ADC was significantly higher compared with NAWM up to 5 years before detection on FLAIR-weighted images (Fig 3*A*; $t[8] = 3.9$, $P = .047$). Similarly, ΔADC was significantly higher than zero up to 5 years before detection (Fig 3*B*; $t(8) = 3.9$, $P = .047$). Increased ADC values within WMLs before detection on FLAIR-weighted images also seemed apparent on FLAIR scans and ADC maps of individual patients who developed new WMLs during the study (Fig 4).

LME modeling revealed that sex had a small-but-significant positive fixed effect on NAWM ADC values, showing a 22.1 (95% CI, 3.7–40.4) $\times 10^{-6}$ mm^2/s higher ADC intercept for men compared with women ($P = .02$; Online Supplemental Data). Neither time, age, nor the presence of lesions had a significant effect on NAWM ADC.

ADC and ΔADC within new lesions were significantly affected by sex, with higher intercepts in men compared with women (60.1 [95% CI, 23.8–96.3] $\times 10^{-6}$ mm^2/s, $P < .01$ and 35.1 [95% CI, 6.0–64.2] $\times 10^{-6}$ mm^2/s, $P = .02$ respectively; Tables 2 and 3). ADC but not ΔADC was also higher and increased faster in older patients, indicated by the fixed effect of age (2.1 [95% CI, 0.6–3.7] $\times 10^{-6}$ mm^2/s/month, $P < .01$) and the interaction effect between age and time (0.04 [95% CI, 0.00–0.07] $\times 10^{-6}$ mm^2/s/year/month, $P = .03$). The effects of time, sex, and age on ADC are shown in Fig 5. ΔADC values increased significantly faster in men compared with women (0.99 [95% CI, 0.27–1.71] $\times 10^{-6}$

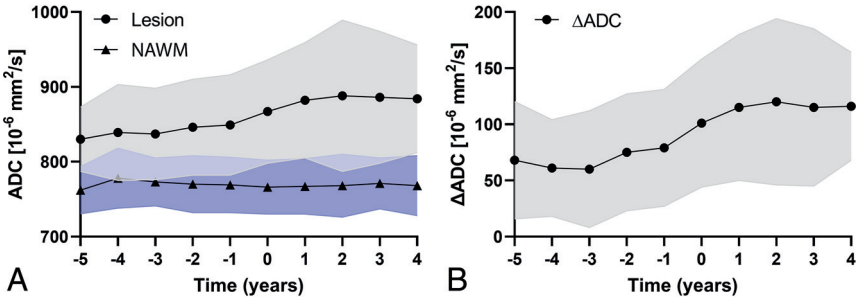

FIG 3. ADC (*A*) and ΔADC (*B*) in new lesion ROIs compared with NAWM. ADC within lesions with the same time (in years) relative to their reference point were combined to calculate mean values (data points) and their SDs (*shaded areas*). For example, ADC_{TP1} within the new lesion TP2 and ADC_{TP2} within new lesion TP3 both have time = −1 but are compared with the HAWM ADC from TP1 and TP2, respectively. Paired *t* tests showed that the ADC within lesions was significantly higher than the ADC within NAWM and that ΔADC was significantly higher than zero at every time. NAWM indicates normal appearing white matter.

mm^2/month, $P < .01$). Time itself had a significant fixed effect only on ΔADC (0.49 [95% CI, 0.03–0.95] $\times 10^{-6}$ mm^2/month, $P = .04$; Online Supplemental Data).

When we evaluated the models using only the TPs before detection, none of the effects describing ADC remained significant, though sex nearly did (35 [95% CI, −3.6–74.5] $\times 10^{-6}$ mm^2, $P = .075$; Tables 2 and 3). For ΔADC, only the significant fixed effect of time remained (0.57 [95% CI, 0.01–1.14] $\times 10^{-6}$ mm^2/month, $P = .047$; Online Supplemental Data).

DISCUSSION

In this 5-year follow-up study, ADC within WMLs of patients with Fabry disease was assessed before and after detection on FLAIR-weighted images in a unique longitudinal data set. ADC values were already increased compared with NAWM in regions that at later TPs were positively identified as WMLs on FLAIR MR imaging. This increase in ADC with time was affected by sex, with men showing a faster increase in ADC than women.

With Fabry disease being an X-linked disease, men are generally more severely affected by it than women. Indeed, this study shows that ADC within WMLs is higher and diverges faster from NAWM values in men compared with women, a finding not observed before.[7,23,24] However, 1 study reported a comparable WML load between men and women, despite the men being younger, suggesting an earlier onset of WMLs in men.[7] A different study comparing diffusivity was limited by its small sample size ($n = 27$), cross-sectional setup, and combined inclusion of classic and nonclassic patients.[24] Although here only slightly more patients with WMLs were included ($n = 33$), the longitudinal design resulted in 472 observations for the analysis.

Higher ADC values were found in regions confirmed as WML at later TPs, consistent with earlier research showing increased diffusivity in NAWM areas commonly associated with WMLs[16] and indicating that changes in diffusion precede WML detection on FLAIR images. When only the TPs before detection were entered into the model, no effects remained statistically significant for ADC. For ΔADC, only time remained statistically significant. This finding may be explained by a lack of statistical power to detect changes in ADC while still detecting ADC increasing faster compared with NAWM. We did not develop a prediction model for WMLs based on ADC but merely showed an association between increased ADC and WML development at later TPs. To determine the predictive value of DWI, a model should be verified using a separate data set. Nevertheless, our findings add to the existing evidence that changes in diffusion precede the formation of WMLs in patients with Fabry disease.

The increasing ADC values with age in WMLs were not observed when considered relative to NAWM (ΔADC). This finding suggests that the observed effect of age is not WML-specific but rather affects WM globally. However, time had no significant effect on NAWM ADC. These ambiguous results emphasize the need for caution when interpreting the NAWM ADC results from this patient population. On the other hand, heterogeneous age-related microstructural alterations across the WM[25] might prevent the observation of a time effect when considering global WM ADC.

A limitation of this study is the absence of an age- and sex-matched control group. Therefore, ADC within lesions could be compared only with NAWM ADC from other brain regions. NAWM ADC values were similar to literature values from healthy control studies (804 [SD, 110] $\times 10^{-6}$ mm^2/s).[26] However, it is possible that WM is affected globally in patients with Fabry disease and that areas detected as lesions are just more severely affected than NAWM. This possibility would align with the pathogenesis of patients with MS as observed in studies using magnetization transfer imaging[27] and DTI.[28] A potential continuation of this study could address this limitation by including a carefully matched healthy control group. Nonetheless, the assessment of diffusion within WMLs both before and after their detection on FLAIR images remained unaffected by the absence of a control group.

All patients included here received ERT, hampering the analysis of the effect of ERT. Treatment duration was explored as a parameter in the LME models but did not yield a statistically significant finding, possibly due to selection bias. Earlier studies reported ambiguous results on the effect of ERT on WMLs. Two studies did not find an effect,[3,29] while a third study found that WML burden was more likely to remain stable in patients on ERT.[30] Although its ability to evaluate ERT is uncertain, this study shows that DWI could still be useful in clinical decision-making. For example, ERT may be delayed until signs of disease progression are observed. In such cases, DWI could serve as a more sensitive marker for detecting early changes. Moreover, if DWI reveals that WMLs continue to progress despite ERT, this finding may be a signal to consider discontinuing the therapy. However, a more thorough validation of the predictive value of DWI must be performed before it can be relied on for such applications.

Some other limitations should be acknowledged. Due to the rarity of the disease, the number of included patients is relatively low, limiting statistical power. However, the longitudinal study

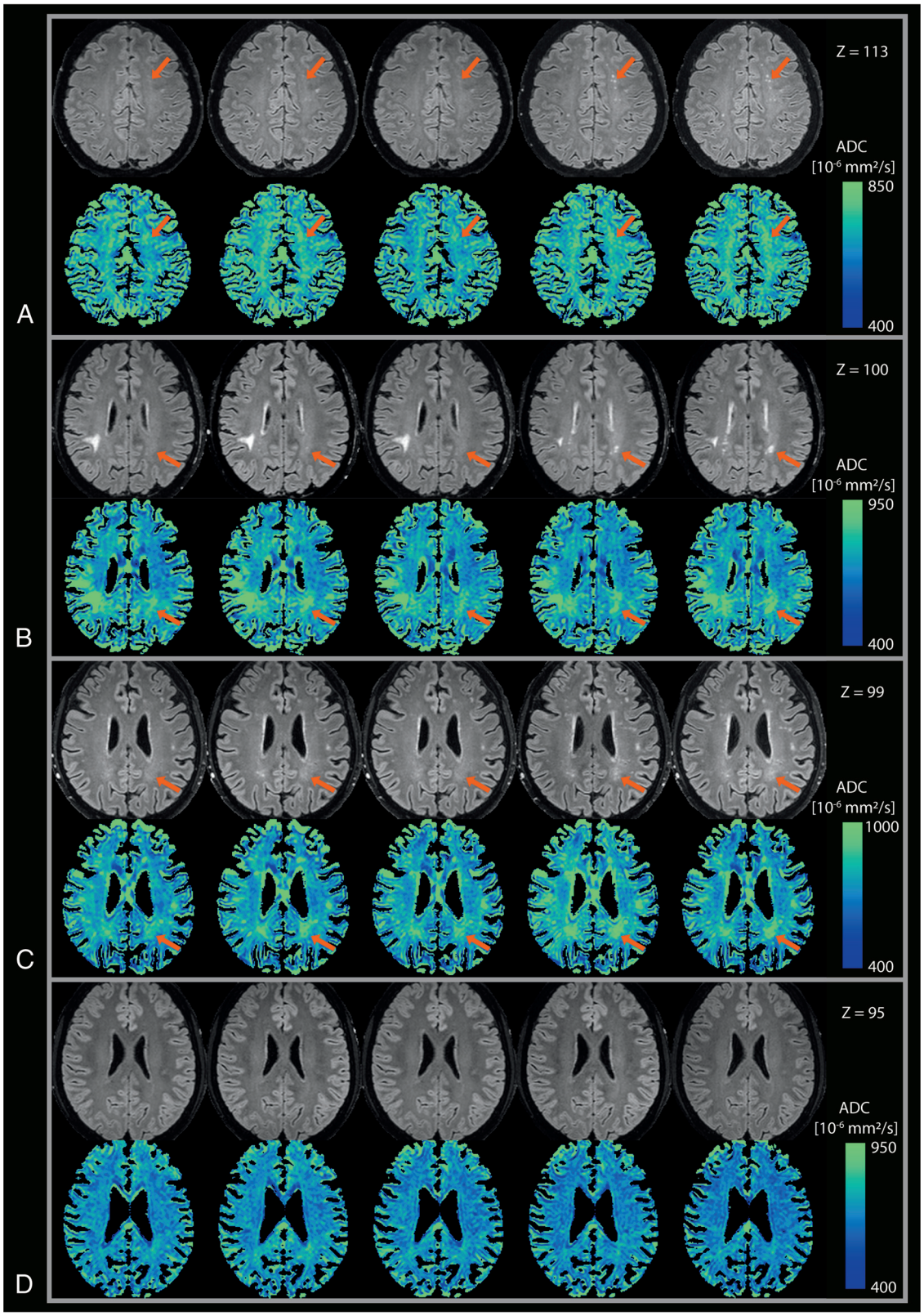

FIG 4. Yearly FLAIR scans and ADC maps. Three of these patients developed WMLs during the study (*A–C*), while 1 patient did not (*D*). Scans are shown in chronologic order from left to right. New WMLs are indicated by the *orange arrows*. The patient in *B* also had a large WM hyperintensity at the right parieto-occipital sulcus, which was diagnosed as a result of infarction before the study. Color scales are optimized for each patient individually. Z values indicate the Z coordinate in standard MNI space.

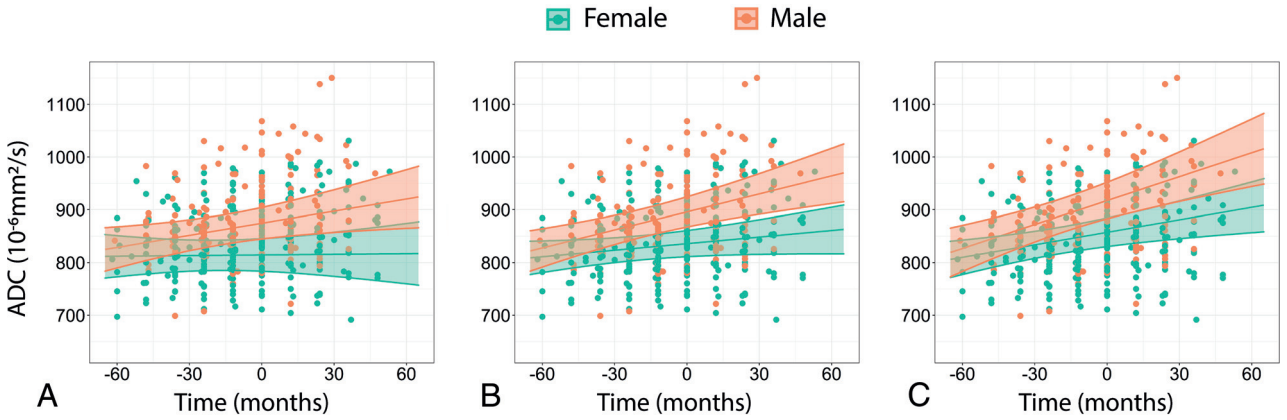

FIG 5. Visualization of LME models describing the ADC within new lesions. The graphs show how time and sex would affect the ADC of 36-, 46-, and 56-year-old patients superimposed on the measured data (*A–C* respectively). ADC is higher and increases faster in men compared with women and increases faster in older patients.

Table 2: Summary of the obtained LME models describing ADC and ΔADC

Predictors	ADC			ΔADC		
	Estimates	CI	*P*	Estimates	CI	*P*
(Intercept)	836	810–862	<.01	84.4	63.1–105.7	<.01
Time (mo)	0.41	−0.08–0.91	.10	0.49	0.03–0.95	.04
Male sex	60.1	23.8–96.3	<.01	35.1	6.0–64.2	.02
Age (baseline, mean centered, year)	2.1	0.6–3.7	<.01	1.10	−0.16–2.36	.09
Time:male sex	0.72	−0.05–1.50	.07	0.99	0.27–1.71	<.01
Time:age	0.04	0.00–0.07	.03	0.03	−0.00–0.06	.09
Observations	472			464		
Marginal R^2	0.227			0.199		
Conditional R^2	0.689			0.613		

Table 3: Summary of the obtained LME models describing ADC and ΔADC before lesion detection on FLAIR-weighted images

Predictors	ADC before Detection			ΔADC before Detection		
	Estimates	95% CI	*P*	Estimates	95% CI	*P*
(Intercept)	834	806–861	<.01	83.2	59.9–106.5	<.01
Time (mo)	0.44	−0.17–1.04	.15	0.57	0.01–1.14	.047
Male sex	35.4	−3.6–74.5	.08	10.7	−21.8–43.1	.52
Age (baseline, mean centered) (yr)	1.0	−0.8–2.8	.25	0.32	−1.22–1.86	.68
Time:male sex	−0.16	−1.10–0.79	.74	0.11	−0.71–0.94	.79
Time:age	−0.00	−0.05–0.05	.85	−0.00	−0.05–0.04	.87
Observations	233			225		
Marginal R^2	0.114			0.035		
Conditional R^2	0.601			0.452		

design partly overcomes this limitation. Given the low sample size, exclusive inclusion of patients with the classic phenotype, and the primary focus on investigating the potential predictive value of DWI, a comparison among patients with different *GLA* gene mutations or phenotypes was not conducted, which remains a topic for future research. Second, because of the large number of MR images, a semiautomated approach was used to segment the WMLs rather than manual segmentation by a trained neuroradiologist. Last, the acquisition protocol used in this study was not initially designed for a scientific investigation but rather for initial exploration, explaining why a more comprehensive technique like DTI was not used in this patient group.

CONCLUSIONS

This work presents the analysis of a unique, longitudinal data set of DWI and FLAIR MR imaging in patients with Fabry disease. Adding to the existing body of literature, these results indicate that changes in diffusion precede the formation of WMLs, suggesting that DWI may be of predictive value for WML formation in Fabry disease. Moreover, these results show that WML diffusivity progresses faster in men compared with women.

ACKNOWLEDGMENT

ChatGPT (https://openai.com/chatgpt) has been used to improve the clarity, grammar, and overall quality of the manuscript.

Disclosure forms provided by the authors are available with the full text and PDF of this article at www.ajnr.org.

REFERENCES

1. Fabry H. **Angiokeratoma corporis diffusum: Fabry disease—historical review from the original description to the introduction of enzyme replacement therapy**. *Acta Paediatr* 2002;91:3–5 CrossRef Medline
2. Zarate YA, Hopkin RJ. **Fabry's disease**. *Lancet* 2008;372:1427–35 CrossRef Medline
3. Jardim LB, Aesse F, Vedolin LM, et al. **White matter lesions in Fabry disease before and after enzyme replacement therapy: a 2-year follow-up.** *Arq Neuropsiquiatr* .2006;64:711–17 CrossRef
4. Körver S, Vergouwe M, Hollak CEM, et al. **Development and clinical consequences of white matter lesions in Fabry disease: a systematic review**. *Mol Genet Metab* 2018;125:205–16 CrossRef
5. Ulivi L, Kanber B, Prados F, et al. **White matter integrity correlates with cognition and disease severity in Fabry disease.** *Brain* 2020;143:3331–42 CrossRef Medline
6. Murphy P, Williams F, Davagnanam I, et al. **Cognitive dysfunction and white matter hyperintensities in Fabry disease.** *J Inherit Metab Dis* 2022;45:782–95 CrossRef Medline
7. Rost NS, Cloonan L, Kanakis AS, et al. **Determinants of white matter hyperintensity burden in patients with Fabry disease.** *Neurology* 2016;86:1880–86 CrossRef Medline
8. Arends M, Wanner C, Hughes D, et al. **Characterization of classical and nonclassical Fabry disease: a multicenter study.** *J Am Soc Nephrol* 2017;28:1631–41 CrossRef Medline
9. Fellgiebel A, Keller I, Marin D, et al. **Diagnostic utility of different MRI and MR angiography measures in Fabry disease.** *Neurology* 2009;72:63–68 CrossRef Medline
10. Rombach SM, Twickler TB, Aerts JM, et al. **Vasculopathy in patients with Fabry disease: current controversies and research directions.** *Mol Genet Metab* 2010;99:99–108 CrossRef Medline
11. Wei EP, Kontos HA, Beckman JS. **Mechanisms of cerebral vasodilation by superoxide, hydrogen peroxide, and peroxynitrite.** *Am J Physiol* 1996;271(3 Pt 2):H1262–66 CrossRef Medline
12. Moore DF, Kaneski CR, Askari H, et al. **The cerebral vasculopathy of Fabry disease.** *J Neurol Sci* 2007;257:258–63 CrossRef Medline
13. Moore DF, Altarescu G, Barker WC, et al. **White matter lesions in Fabry disease occur in "prior" selectively hypometabolic and hyperperfused brain regions**. *Brain Res Bull* 2003;62:231–40 CrossRef Medline
14. Böttcher T, Rolfs A, Tanislav C, et al. **Fabry disease: underestimated in the differential diagnosis of multiple sclerosis?** *PLoS One* 2013;8:e71894 CrossRef Medline
15. Albrecht J, Dellani PR, Müller MJ, et al. **Voxel based analyses of diffusion tensor imaging in Fabry disease**. *J Neurol Neurosurg Psychiatry* 2007;78:964–69 CrossRef Medline
16. Paavilainen T, Lepomäki V, Saunavaara J, et al. **Diffusion tensor imaging and brain volumetry in Fabry disease patients**. *Neuroradiology* 2013;55:551–58 CrossRef Medline
17. Körver S, Longo MG, Lima MR, et al. **Determinants of cerebral radiological progression in Fabry disease**. *J Neurol Neurosurg Psychiatry* 2020;91:756–63 CrossRef Medline
18. Tol van der L, Cassiman D, Houge G, et al. **Uncertain diagnosis of Fabry disease in patients with neuropathic pain, angiokeratoma or cornea verticillata: consensus on the approach to diagnosis and follow-up**. *JIMD Rep* 2014;17:83–90 CrossRef Medline
19. Smid BE, Van Der Tol L, Cecchi F, et al. **Uncertain diagnosis of Fabry disease: consensus recommendation on diagnosis in adults with left ventricular hypertrophy and genetic variants of unknown significance.** *Int J Cardiol* 2014;177:400–08 CrossRef Medline
20. Schmidt P. **Bayesian Inference for Structured Additive Regression Models for Large-Scale Problems with Applications to Medical Imaging.** *Mathematics* January 17, 2017. https://www.semanticscholar.org/paper/Bayesian-inference-for-structured-additive-models-Schmidt/edc315de56ff336b75f36b30bad74fab231d39ca. Accessed June 20, 2022
21. Bates D, Mächler M, Bolker BM, et al. **Fitting linear mixed-effects models using lme4**. *Journal of Statistical Software* 2015;67 CrossRef
22. Baayen RH, Davidson DJ, Bates DM. **Mixed-effects modeling with crossed random effects for subjects and items.** *Journal of Memory and Language* 2008;59:390–412 CrossRef
23. Fellgiebel A, Müller MJ, Mazanek M, et al. **White matter lesion severity in male and female patients with Fabry disease**. *Neurology* 2005;65:600–02 CrossRef Medline
24. Fellgiebel A, Mazanek M, Whybra C, et al. **Pattern of microstructural brain tissue alterations in Fabry disease: a diffusion-tensor imaging study.** *J Neurol* 2006;253:780–87 CrossRef Medline
25. Burzynska AZ, Preuschhof C, Bäckman L, et al. **Age-related differences in white matter microstructure: region-specific patterns of diffusivity**. *Neuroimage* 2010;49:2104–12 CrossRef Medline
26. Sener RN. **Diffusion MRI: apparent diffusion coefficient (ADC) values in the normal brain and a classification of brain disorders based on ADC values.** *Comput Med Imaging Graph* 2001;25:299–326 CrossRef Medline
27. Filippi M, Campi A, Dousset V, et al. **A magnetization transfer imaging study of normal-appearing white matter in multiple sclerosis.** *Neurology* 1995;45:478–82 CrossRef Medline
28. Ciccarelli O, Werring DJ, Wheeler-Kingshott CA, et al. **Investigation of MS normal-appearing brain using diffusion tensor MRI with clinical correlations.** *Neurology* 2001;56:926–33 CrossRef Medline
29. Jardim L, Vedolin L, Schwartz IV, et al. **CNS involvement in Fabry disease: clinical and imaging studies before and after 12 months of enzyme replacement therapy.** *J Inherit Metab Dis* 2004;27:229–40 CrossRef Medline
30. Fellgiebel A, Gartenschläger M, Wildberger K, et al. **Enzyme replacement therapy stabilized white matter lesion progression in Fabry disease**. *Cerebrovasc Dis* 2014;38:448–56 CrossRef Medline